

# Dorsal Hand Vein Identification Based on Binary Particle Swarm Optimization

Sarah Hachemi Benziane<sup>\*,\*\*</sup> and Abdelkader Benyettou\*

## Abstract

The dorsal hand vein biometric system developed has a main objective and specific targets; to get an electronic signature using a secure signature device. In this paper, we present our signature device with its different aims; respectively: The extraction of the dorsal veins from the images that were acquired through an infrared device. For each identification, we need the representation of the veins in the form of shape descriptors, which are invariant to translation, rotation and scaling; this extracted descriptor vector is the input of the matching step. The optimization decision system settings match the choice of threshold that allows accepting/rejecting a person, and selection of the most relevant descriptors, to minimize both FAR and FRR errors. The final decision for identification based descriptors selected by the PSO hybrid binary give a FAR =0% and FRR=0% as results.

## Keywords

Biometrics, BPSO, GPU, Hand Vein, Identification, OTSU

## 1. Introduction

The use of the word biometrics refers increasingly to the use of these techniques for purposes of identification/authentication, the first sense of the word biometrics then being taken over by the term Biostatistics. The biometrics word has a larger meaning in the study of identification/authentication persons from a number of characteristics. It is a Mathematical analysis of biological and/or behavioral characteristic of a person to determine his identity decisively. Biometric modalities are based on principle characteristics recognition as fingerprint [1], face [2], iris [3], retina [4], hand [5], keystroke, voice and vein; they provide irrefutable proof of the identity of a person by their biological uniqueness characteristics distinguishing one person from another. The hand vein biometrics has emerged as a promising component of the biometric study [6-9]. Each biometric system has a processing chain, including the hand vein system in order to obtain a final decision [10]. The biometric vein profile has a very high level of security, so far there is no means of fraud, this type of biometry is called “contactless”. The rest of the paper is organized as follows: we will briefly introduce prior researches relevant to Hand vein biometric.

\* This is an Open Access article distributed under the terms of the Creative Commons Attribution Non-Commercial License (<http://creativecommons.org/licenses/by-nc/3.0/>) which permits unrestricted non-commercial use, distribution, and reproduction in any medium, provided the original work is properly cited.

Manuscript received January 6, 2016; first revision April 5, 2016; accepted May 11, 2016.

Corresponding Author: Sarah Hachemi Benziane (sarah\_benziane1@yahoo.fr)

\* Dept. of Computer Science, SIMPA Laboratory, University of Science and Technology of Oran-Mohamed Boudiaf, Oran, Algeria (a\_benyettou@univ-oran.dz)

\*\* Institute of Maintenance and Industrial Safety, IMSI, University of Oran 2, Algeria (sarah.benziane@univ-oran.dz)

In Section 2, a detailed description of the proposed system; Section 3 presents enhancement of the quality of the database used for better vein feature extraction which is detailed in Section 4. Section 5 show how to get the vector feature extraction. Section 6, gives a brief description about the hybridization of the BPSO. Section 7 presents the experimentation and results of the proposed system; prior to conclusions in Section 9.

In visible light, the veins are not apparent. Indeed, a multitude of other factors, including the surface characteristics such as moles, warts, scars, pigmentation and hair can also hide the image [11]. Fortunately, the use of the infrared light eliminates most unwanted surface features [12]. Required parameters to obtain good quality data are listed below [11,13]:

- The light affects the quality of the image obtained with the exception of no IR filter.
- The temperature of the ambient environment must be neither too hot nor too cold, around the human body temperature.
- The distance between the sensor and the object should be sufficient for a good acquisition.

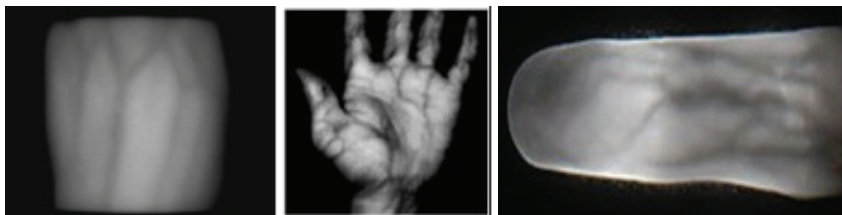


**Fig. 1.** Dorsal, palmar and fingerprint veins.

Starting with Jackson W. Wegelin patent [14], includes a dispenser controller coupled to a memory unit, which includes a database of previously-stored vein patterns. A vein-pattern sensor maintained by the dispenser images the unique vein pattern of a user's hand without contact. A recent study proposed using a three dimensional biometric scanner: (1) for the capillary mapping of the palm of the hand (2) incorporates two image sensors; configured for obtaining a stereoscopic image of a vascular map and where for each image corresponding to each wave length, the depth of each point on the plane is known [15]. Some multimodal biometric systems capture palmprint/finger vein [16,17] like shown Fig. 1, hand geometry/vein [18,19]. Other systems capture the palmar veins [20,21] Based on registering finger vein information [22], and it is discriminated of which finger the finger vein information is to be registered, on the basis of the photographed image. There is too central combining several modalities as [23] which comprise a central command station in signal communications with a series of blasting machines. Command station has a biometric analyser unit and an authorizing means. The blasting apparatuses have enhanced security features by including biometric analysis of specific biological features of an authorized blast operator to generate a known biometric signature. The biometric signature can be derived from a fingerprint scan, a recognition scan of a hand, a foot, an iris or a retina, a skin spectroscopy analysis, a finger vein pattern analysis, a voice recognition analysis, or a DNA fingerprint analysis. In order to get areas, improve the quality of the image, extract veins from hand, we need some techniques:

a) Format conversion JPEG BMP: the conversion JPEG BMP is required. Indeed, the main advantage of BMP image quality is provided as BMP format is not compressed and therefore no loss of quality. Against by the JPEG format is compressed and therefore quality lost [24].

b) Enhancement: The resulting image may not contain noise as tasks, blobs, dust, etc. Different filters can be applied to eliminate the noise and enhance the image, but if the pictures have a good quality, this step is not required [25]. In [26], the clearness of the vein pattern in the extracted ROI (region of interest) varies from image to image; they use a  $5 \times 5$  Median Filter to remove the speckling noise in the images and a 2-D Wiener filter to the ROI image to suppress the effect of high frequency noise. [27] uses a various contrast enhancement techniques in order to compare which gives the best results, the study is very interesting.

c) Converting the color image into a gray level: Converting a color image into a grayscale means that the image size will be reduced from 24 bits per pixel (color image) to 8 bits per pixel (grayscale image) [14,28]. Instead of having three matrices that represent the level of colors (red, green, blue) for each pixel, we have just a single matrix that represents the gray level for each pixel, which reduces the processing time [29,30].

d) Binarization is segmenting the image into two levels; object (hand region) and background; most of the time the object segment which is the ROI in white and the background segment in black [31-33]. After the binarization, there is the most difficult step which is the feature extraction. Some researchers add a step in this phase [24,28,33,34]. Some works use the minutiae features extracted from the vein patterns for recognition, which include bifurcation points, ending points and the position and orientation of minutiae points [35,36]. [37,38] uses it with the vein finger, when [26] uses it with the dorsal hand vein. In [32], the feature extraction was based on the geometry veins. Fig. 2 shows these minutiae (playback direction: from left to right).

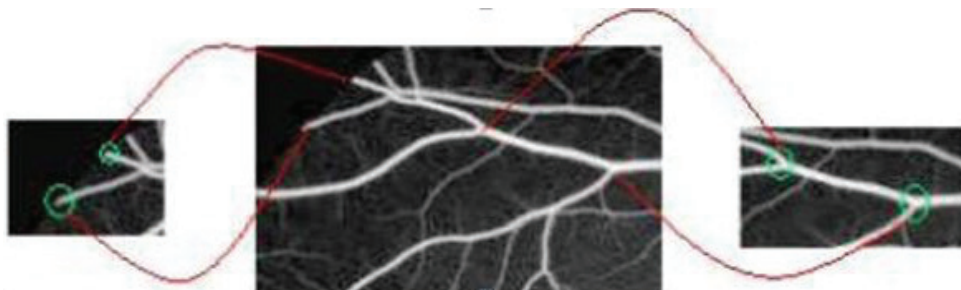


**Fig. 2.** End points, veins branching points [37].

e) Identification/authentication phase or then verification is only classification [39,40] of items into two classes. The image of the veins that was extracted in the previous step allow us to create a database of prototypes with pattern that are in the database (template) by authenticating the identity of an individual, will either accept the person, or reject it. Instead of the identification [41,42], the system will identify the right person. In order to evaluate their system testing performance, [31] uses a dataset of 500 persons of different ages above 16 and of different gender, each has 10 images per person was acquired at different intervals, 5 images for left hand and 5 images for right hand. [43] used correlation and template matching as a recognition algorithm whether [44] used Principle Component Analysis (PCA). The authors [45,46] present a general survey on the hand biometrics; some of the works quoted are summarized in Table 1.

**Table 1.** Survey of hand vein biometrics

Ref.	Dimension	Thresholding	Binarization	Vein extraction	Minutiae's extraction	Classification	Number dataset	Performance
[47]	160x120	Gaussian low	Local	Local	No		10.000	FAR 0.01%
[35]		Pass and high pass	Thresholding	Thresholding				
[48]	Combination	Median	Local	Wavelet	No		30	FRR 1.5%
[38]	Multi resolution		Thresholding	Transform				FAR 3.5%
[49]		Median	Local	Local	No	Hausdorff	12	FRR 0%
[24]		Gaussian	Thresholding	Thresholding		Distance		FAR 3.0%
[50]		GSZ	No	Gabor	Cross	KNN with		
[33]		Shock		Thresholding	number	Euclidean		
[22]	640x480	Median	Threshold=0	Skeletonisation				
[37]	Special median							
[28]	640x320	Gaussian	SIFT	SIFT		Euclidian	24	EER 0%
[6]		Low pass				Distance		

## 2. Proposed System Description

This paper deals with a new biometric identification approach. The main contributions of this paper can be summarized as follow:

- Representation of the veins vector in the form of shape descriptors, they are invariant to translation, rotation and scaling. The classification is done based on these descriptors.
- Optimization decision system settings match the choice of threshold that allows to accept/reject a person, and selection of the most relevant descriptors, to minimize both FAR and FRR errors.
- The integration of hybrid binary PSO for solving the bi-objective optimization problem (FAR and FRR minimized). This meta-heuristic decision provides greater credibility by introducing the notion of subjective parameters (formulated by the decision maker), corresponding to the weight assigned to the FAR and FRR.
- Identification based descriptors selected by the PSO hybrid binary.

From The dorsal vein hand image are extracted contours used for the image normalization and segmentation of ROI which is detailed in Sections 2. The extraction of hand vein vector from ROI images is described in Section 3. The extraction feature from the hand vein vector and the identification are detailed in Sections 4 and 5, respectively. The experiments and results of this work are presented in Section 5, which is followed by the discussion in Section 6.

The main architecture of our identification biometric system consists of three modules: enhancement module, feature extraction, and classification (Fig. 3). The first two modules were implemented on CPU.

The functional architecture of the decision system matches the biometric identification with dorsal hand vein developed; is shown below.

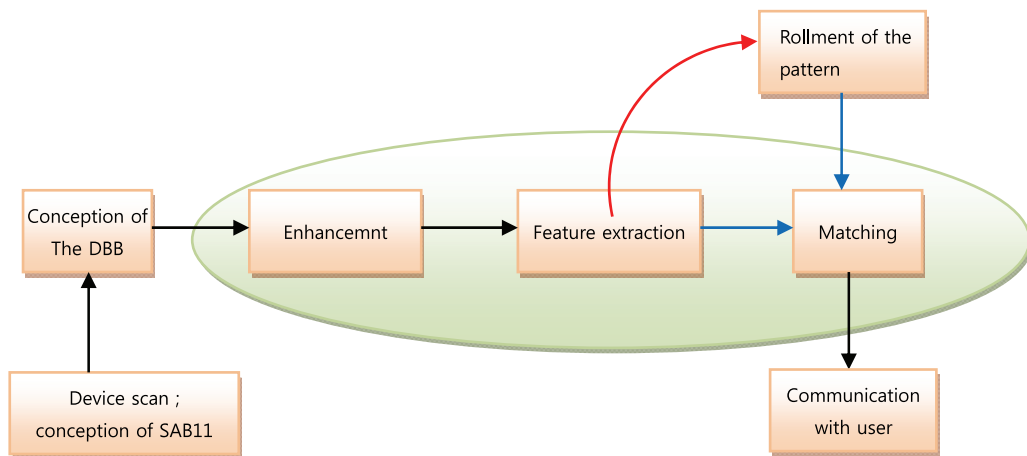


**Fig. 3.** Block diagram of our decision support system.

### 3. Image Quality Amelioration

The NCUT databases images are images taken of the hands at a distance. Thus, the image is composed of two parts by hand and background surrounding To avoid wasting time calculation by processing a non interesting area which is the background of the image. We get extraction of the area (two segments) by applying a binarization. This step allows us to divide the image in two areas: the hand area (white) and the background (black). We used the OTSU's algorithm below:

#### Algorithm 1. OTSU for the binarization

```

Upload image;
Convert from color to grayscale;
Calculate the histogram of the image;
Normalization of the histogram;
Mean (0) =0;
Var (0) =0;
If k<= 255
    Update mean (k);
    Update car (k);
    Calculate  $S^2(K)$ ;
Else
    Threshold Binarization, T=k
     $S^2(k)=\max(S^2(k))$  ;
    If  $I(x,y)>T$ 
         $I(x,y)>T=1$ 
    Else
         $I(x,y)>T=0$ 

```

Since the background is useless, we must eliminate it and keeping only the white pixels in the image that is to say; the area of the hand (see Fig. 4).



**Fig. 4.** Binarization for hand area extraction.

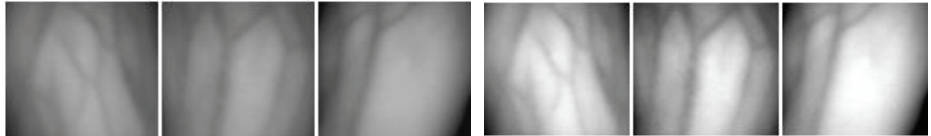


**Fig. 5.** Extraction and enhancement.

In order to extract the area of interest (ROI) that contains the veins, we calculated the gravity hand center; as shown in Eqs. (1) and (2). this operation aims to eliminate the bottom (the image size reduction) and have more accurate results.

$$X_g = \frac{\sum_{i,j} i * I(i,j)}{\sum_{i,j} I(i,j)}; \quad (1)$$

$$Y_g = \frac{\sum_{i,j} j * I(i,j)}{\sum_{i,j} I(i,j)} \quad (2)$$

as the images of the veins were not clearly distinguished; we improved the contrast by a linear transformations. Linear transformation includes simple identity and negative transformation. Identity transition is shown by a straight line. In this transition, each value of the input image is directly mapped to each other value of output image. That results in the same input image and output image. And hence is called identity transformation. The results of different people are shown in Fig. 5.

From the work done on the analysis and the investigation of images on the pre-processing operations, the final image pre-processing system is proposed to consist of four steps, namely the extraction of the ROI, Grayscale normalization, anisotropic diffusion filter [51] and adaptive equalization of the histogram to improve contrast.

## 4. Vein Feature Extraction

Once we extract ROI, we proceeded to a binarization thresholding operation to divide the image into two levels: black background and white veins, by the method of integral image. Based on the following Algorithm 2.

The problem with this method was how to choose the size of the window ( $w \times w$ ) and coefficient  $k$ . The integral image is used as a quick and effective way of calculating the sum of values (pixel values) in a given image – or a rectangular subset of a grid (the given image). It's why we applied several tests in the size of the window, setting  $k=0$  on several people. Fig. 6 shows the results for the same person.

**Algorithm 2.** The integral image for binarization

---

Calculating the integral of all images (with H the height and L the width);  
 Compute the new center (x, y) of the window;  
**if**  $x < H$   
 Calculating the local sum of the integral;  
 Calculating the local mean;  
 Calculates the standard deviation;  
 Calculates the threshold T for the center of the window;  
**If**  $I(x,y) > T$   
 $I(x,y) > T = 1$   
**Else**  
 $I(x,y) > T = 0$

---



**Fig. 6.** Binarization by integral image for the extraction of dorsal hand veins.

From the results, we found that the window size with (55×55) gave us the best visualization of the veins, so we took the window size (55×55) and coefficient  $k=0$  for binarization. To improve the quality of the binary image, we applied the morphological dilation operation, which will allow us to remove black areas of the image. The results are shown in Figs. 7 and 8.

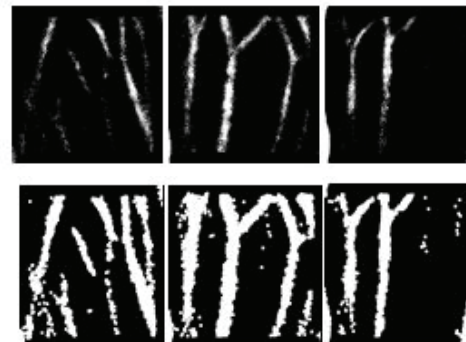


**Fig. 7.** Before and after dilation with (7×7).

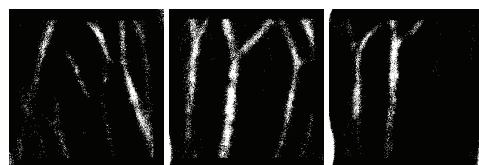


**Fig. 8.** Vein binary image after dilatation.

According to the results, we noticed that there still have isolated pixels, so it must be eliminated by applying a filter. We chose the Median filter because usually it is the response filter. However, its performance is not that much better than Gaussian blur for high levels of noise, whereas, for speckle noise and salt and pepper noise (impulsive noise), it is particularly effective. Furthermore, some types of signals (very often the case for images) use whole number representations; in these cases, histogram medians can be far more efficient because it is simple to update the histogram from window to window, and finding the median of a histogram is not particularly onerous. The results are shown in Fig. 9.



**Fig. 9.** Vein binary image after dilatation window (7×7).

## 5. Vector Feature Extraction

This step is intended to represent the veins by color descriptors, texture, shape, or the combination of both these descriptors. since the comparison between the images is done by these descriptors. For this, we chose the shape descriptors, cause they are invariant to rotation, translation and scaling. We opted for the method of HU moment invariants, which will extract seven descriptors of shapes, from the binary images of dorsal veins of the hand. The corresponding organigram is presented in Fig. 10.

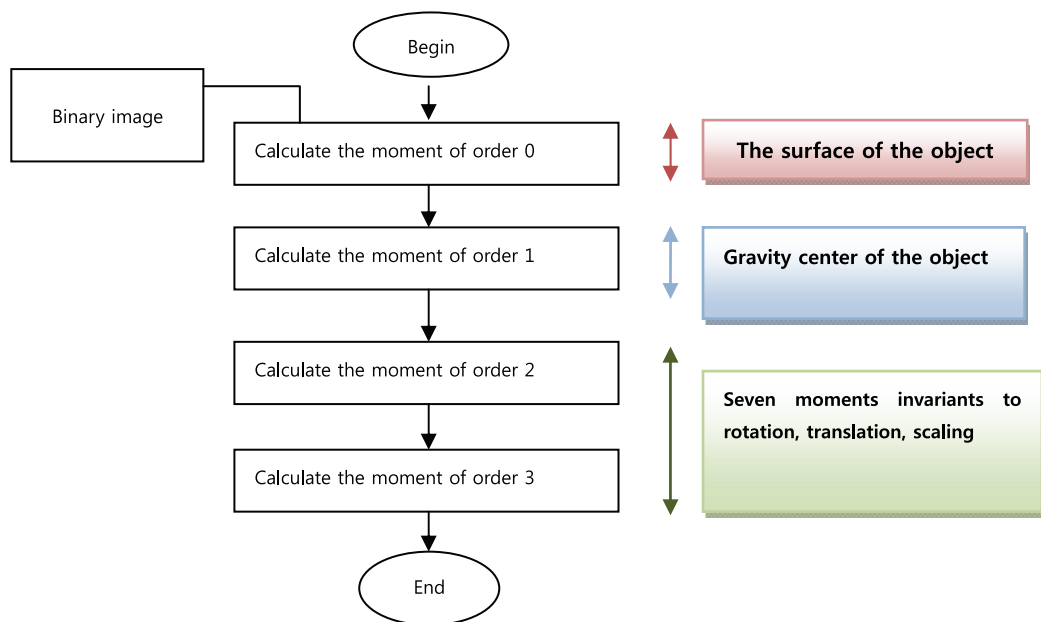


**Fig. 10.** Feature extraction by the method of moment invariants HU.

## 6. Hybridization of BPSO with Moment Invariants HU

The disadvantage of the seven Hu moment invariants is that they are sensitive to noise, in addition they are very hungry time calculated. So in order to select only the moments that minimize both FAR and FRR errors, we will make a hybridization of BPSO (binary PSO) with the method of invariant moments of HU. This hybridization has two main goals:

- Select less time instead of seven times like shape descriptors dorsal hand veins, which minimize both errors FAR and FRR.
- To have an optimal threshold that can accept or reject people.

This hybridization was never done before. It is presented as follows:

Step 1: Initialize settings BPSO (N: the number of particles the number of iterations).

Step 2: Initialize the positions X and speed V.

$$X = \begin{pmatrix} x_{11} & x_{12} & \dots & x_{iM} \\ x_{21} & x_{22} & \dots & x_{iM} \\ \cdot & \cdot & \cdot & \cdot \\ \cdot & \cdot & \cdot & \cdot \\ x_{N1} & x_{N2} & \dots & x_{iM} \end{pmatrix}$$

$$x_{im} = \text{randint}()$$

$$V = \begin{pmatrix} v_{11} & v_{12} & \dots & v_{iM} \\ v_{21} & v_{22} & \dots & v_{iM} \\ \cdot & \cdot & \cdot & \cdot \\ \cdot & \cdot & \cdot & \cdot \\ v_{N1} & v_{N2} & \dots & v_{iM} \end{pmatrix} \quad (3)$$

$$v_{im} = -vmax + 2vmax * rand() \quad (4)$$

where,

$i$  is the particle index

$m$  the  $m^{\text{th}}$  dimension

$x_{im}$  the  $m^{\text{th}}$  selected time of particle  $i$

$\text{randint}()$  means that the moment has been selected 0 else

$M$  the number of selected moment; in our case  $M=7$

$N$  the number of particules

$vmax$  the number of changement; in our case = 7 invariant moments  $\text{rand}() \in [0,1]$

Step 3: The comparison of the images are made on the basis of moments that were selected by BPSO according to the chart below, every person in our case is a class.

Step 4:

**Algorithm 3.** The classification by the hybridation

Upload Input class(binary vein image)

Extraction of the seven invariant moment of Hu

Selection of the moment by BPSO

Calculate  $d1$ : Distance between the input class and all DBB classes

Find the minimal Class  $C$

Separate class  $C$  into two groups, and calculating the distance  $d2$  between them by the  $Dist$  if  $\frac{d1}{d2} \leq T$

where the distance between the images of each person and different people (classes) is calculated by the following equation:

$$Distance = \frac{1}{n_1 * n_2} \sum_{i=1}^{n_1} \sum_{j=1}^{n_2} dist(A_i; B_j) \quad (5)$$

where  $n_1$  and  $n_2$  are the number of an image in class A and B, respectively,  $dist(A_i; B_j)$  is the Euclidean distance between the image  $A_i$  and the class B.

Step 5: Update the fitness function of each particle, which has two objectives: minimize FAR error (the false acceptance rate) and minimize FRR error (the false rejection rates).

The corresponding function is

$$MinimizeE = CFA * GFAR + CFR * GFRR \quad (6)$$

$$CFR = 2 - CFA \quad (7)$$

where the parameters of the function fitness are defined as:

GFAR is FAR

GFRR is FRR

CFA is the cost of false acceptance

CFR is the cost of false reject

EER is the error rate

Both the FAR and FRR objectives are defined by the following equation:

$$FRR = \frac{\text{Number of rejected genuine}}{\text{Total genuine who accessed}} * 100 \quad (8)$$

$$FAR = \frac{\text{Number of impostors accepted}}{\text{Total impostors who accessed}} * 100 \quad (9)$$

Step 6: If the fitness function of each particle is better than the previous best fitness function, then the current position is the best previous position and the current fitness function is its previous best fitness function.

Step 7: Assign the minimum fitness function all the best fitness functions of each particle, the overall fitness function. The positions of this function will be assigned to the best overall position.

Step 8: Update the speed.

Step 9: Update position.

Step 10: Repeat steps 3, 4, 5, 6, 7, 8 until stopping criterion.

## 7. Experimentation and Results

The information about the database that we used were acquired from the NCUT Database [52]. The information about the database used are summarized in Table 2.

**Table 2.** Database information

Parameter	Definition
Number of person in the DBB	102 (52 women, 50 men)
Number of image per person	10 for the right and for the left hand
Number of image in the DBB	2,040
Number of person (class) for the training	50 (6 images for each person) and the remaining for the test

**Table 3.** Parameters used

Number of iterations	50
Number of particle	10
$c_1$	0.9
$c_2$	1
$w_{max}$	1.9
$w_{min}$	0.4
$r_1$	0.5
$r_2$	0.5

The parameters used in this experiment for BPSO are summarized in Table 3.

For the fitness function, we varied the cost of CFA in the range [0.1,1.9] and the threshold that allows to know if it is a genuine or fake. Figs. 11–13 show the error evaluation FAR, FRR and the objective function (error rate) during the variation of the threshold.

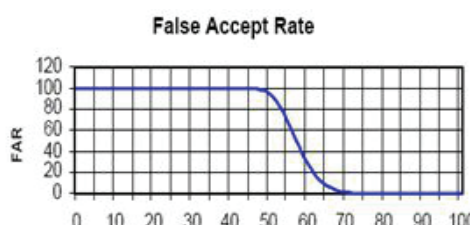


**Fig. 11.** False accept rate (FAR).

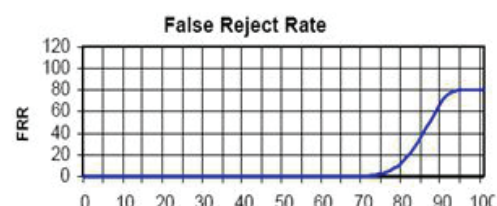


**Fig. 12.** False reject rate (FRR).

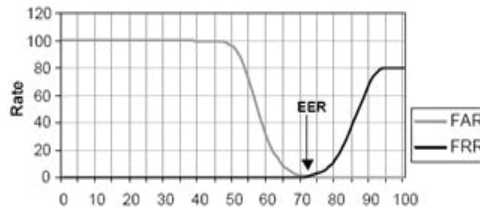


**Fig. 13.** Equal error rate (EER).

Through the histogram in Figs. 11–13, the two errors FAR and FRR were equal with the threshold value is 72%. The results obtained by the hybridization of BPSO with Hu moment invariants for the selection of the best times that minimize both FAR and FRR errors are listed in Table 4.

From the table above, the results obtained by hybridization of BPSO and Hu moment invariants, were able to reach a figure of 0% for both FAR and FRR errors with less time selected instead of seven and a threshold of 72% by varying the CFAR and CFRR. Another remark cost, we observed from the table above, is that the moments ( $\theta_1; \theta_2$ ) were the most selected by BPSO times, so for confirm that, we did a manual selection times with or without these two moments ( $\theta_1; \theta_2$ ).

The results are shown in Table 4.

**Table 4.** Results of HU moment invariants selected by BPSO

CFA	$\theta_1$	$\theta_2$	$\theta_3$	$\theta_4$	$\theta_5$	$\theta_6$	$\theta_7$	FAR	FRR	EER
0.1	1	0	0	1	0	1	0	0	0	0
0.3	0	1	1	1	0	0	1	2	0	0.6
0.4	1	1	1	1	0	0	0	0	0	0
0.6	0	1	1	1	1	1	0	0	0	0
0.9	0	1	1	1	1	0	0	0	0	0
	1	1	1	1	0	0	1	0	0	0
0.6	1	1	1	1	1	0	1	0	0	0
0.9	1	1	0	0	0	0	0	0	0	0
Mean	0.73	0.73	0.68	0.69	0.57	0.36	0.57	0	0	0

From Table 4, we see that the absence of one of these two moments or both, or their presence with both other times the error rate increases. However, the presence of only these two times both the error rate becomes 0%. Therefore, we have taken only two times ( $\theta_1; \theta_2$ ) to represent the veins by two shape descriptors.

## 8. System on GPU

In this section, we will illustrate the implementation of the classification on GPUs, based on the Framework JOCL. The matching algorithm is in Algorithm 3, removing the part selection times by BPSO and threshold variation. Only the distance calculation by Eq. (5) between the images of the veins of the person we have just identified with those in the database will be done on the GPU.

We remind, that each image of the dorsal vein of the hand of a person, is now represented by two values corresponding to both Hu ( $\phi_1, \phi_2$ ) moment invariants, as shown in Fig. 14.

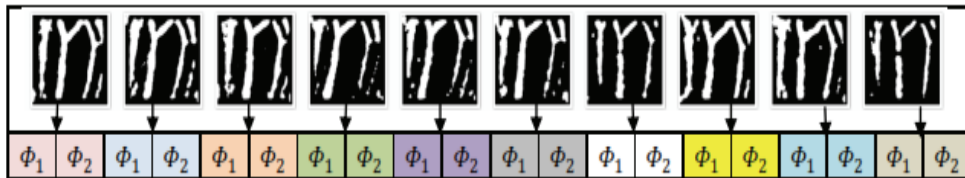


**Fig. 14.** Representation of each image of the dorsal veins of a person as two moments in a single linear array.

#### Algorithm 4. Classification on GPU

**Begin**

- Choose the framework ()
- Choose the type of the device
- Create a context
- Create the waiting thread by the JOCL
- Allocation of the memory for the input and the output data
- Call the kernel program
- Execute the kernel
- Recover the results
- Freeing memory

**End**

Now, to classify this person, we will detail our approach to the implementation of the classification step GPU, by the following chart.

Algorithm 4 shows the communication between the CPU (Host) and the GPU: the input table is an array that contains the value of both Hu moment invariants, for each image of the veins of the person we have just identified. The table of users: it is an array that contains the value of both Hu moment invariants for each image, each person who exists in the database.

For a vein image recognition based on structural features, a new method is proposed based on the hybridization of invariant moments and BPSO. For the recognition of the image of the main-dorsal vein based on the vein network feature, work has led to two proposed approaches based on the vein structure model to control the contribution of BPSO and PCA in recognition. Which proves to provide the highest recognition rate of almost 100%, 99% for the BPSO and the PCA respectively. In this work area, although a wavelet domain approach has also been studied, it has not been included in this paper because it is more intensive in calculation. It is particularly noteworthy to emphasize that structural features based on BPSO and PCA have not previously been applied to the recognition of venous images and the work reported in this paper is considered to represent a summary study on recognition rates Achievable for the BPSO and PCA classification based on dorsal vein images.

## 9. Conclusion

A complete image pre-processing chain has been proposed, which consists of a ROI extraction, gray-scale normalization, anisotropic diffusion filter and contrast-limited adaptive histogram equalization.

Each step was designed and developed using quantitative and qualitative performance assessments in relation to several other approaches. A somewhat new work in this field includes the improvement of the image coherence by means of a simple relative geometric pre-treatment based on the method of extracting the ROI based on a centroid and a coherent with less geometric variations.

According to both measurement error rates FAR and FRR, we get the best results with an error rate FAR=0% and FRR=0% among the work done. According to the execution time, we cannot compare our results to 100% because it depends on the type of used machine. In addition a few studies which have mentioned the execution time of the preprocessing step, feature extraction and classification. Indeed, in biometrics, the authors focus primarily on minimizing both error rate FAR and FRR, after the execution time for biometrics is a type of soft real-time, that is to say, even if there's a delay in obtaining the result will not cause damage. However, it is clear to point out some very important aspects we have deduced by this project. It is not necessary to make the dorsal veins as skeletons to extract minutiae, because this makes it very heavy preprocessing. In addition, once again it is difficult to extract the minutiae of the dorsal hand veins, because of the infrared camera quality used to acquire images of veins. b. May decrease the performance of FAR perspective FRR system, because if one of the minutiae algorithm does not detect it, we will file it in another category.

## References

- [1] C. Pintavirooj, F. S. Cohen, and W. Lampa, "Fingerprint alignment based on local feature combined with affine geometric invariant," in *Proceedings of 18th International Conference in Central Europe on Computer Graphics, Visualization and Computer Vision in co-operation with EUROGRAPHICS*, Plzen, Czech Republic, 2010, pp. 173-178.
- [2] M. Monwar, S. Rezaei, and K. Prkachin, "Eigenimage based pain expression recognition," *IAENG International Journal of Applied Mathematics*, vol. 36, no. 2, pp. 1-6, 2007.
- [3] C. C. Teo and H. T. Ewe, "An efficient one-dimensional fractal analysis for iris recognition," in *Proceedings of the 13th International Conference in Central Europe on Computer Graphics, Visualization and Computer Vision 2005 in co-operation with EUROGRAPHICS*, Plzen, Czech Republic, 2005, pp. 157-160.
- [4] D. N. Antequera and Delrios Sanchez, "3d biometric scanner," EP20,090,842,118, Feb. 1, 2012.
- [5] V. Sasikala, "Bee swarm based feature selection for fake and real fingerprint classification using neural network classifiers," *IAENG International Journal of Computer Science*, vol. 42, no. 4, pp. 389-403, 2015.
- [6] N. Miura, A. Nagasaka, and T. Miyatake, "Feature extraction of finger-vein patterns based on repeated line tracking and its application to personal identification," *Machine Vision and Applications*, vol. 15, no. 4, pp. 194-203, 2004.
- [7] A. K. Jain, A. Ross, and S. Prabhakar, "Fingerprint matching using minutiae and texture features," in *Proceedings of the International Conference on Image Processing*, Atlanta, GA, 2001, pp. 282-285.
- [8] M. H. Wang and Y. K. Chung, "Applications of thermal image and extension theory to biometric personal recognition," *Expert Systems with Applications*, vol. 39, no. 8, pp. 7132-7137, 2012.
- [9] B. W. Beenau, D. S. Bonalle, S. W. Fields, W. J. Gray, C. Larkin, J. L. Montgomery, and P. D. Saunders, "Hand geometry biometrics on a payment device," US Patent 8,289,136, Oct. 16, 2012
- [10] R. Kavitha and L. Flower, "Localization of palm dorsal vein pattern using image processing for automated intra-venous drug needle insertion," *International Journal of Engineering Science & Technology*, vol. 3, no. 6, pp. 4833-4838, 2011.

- [11] M. Rajalakshmi, R. Rengaraj, and P. G. Student, "Biometric authentication using near infrared images of palm dorsal vein patterns," *International Journal of Advanced Engineering Technology*, vol. 2, no. 4, pp. 384-389, 2011.
- [12] L. Wang and G. Leedham, "Near-and far-infrared imaging for vein pattern biometrics," in *Proceedings of IEEE International Conference on Video and Signal Based Surveillance*, Sydney, 2006, pp. 52–52.
- [13] M. M. Pal and R. W. Jasutkar, "Implementation of hand vein structure authentication based system," in *Proceedings of 2012 International Conference on Communication Systems and Network Technologies (CSNT)*, Rajkot, India, 2012, pp. 114–118.
- [14] K. Jain, L. Hong, S. Pankanti, and R. Bolle, "An identity-authentication system using fingerprints," *Proceedings of the IEEE*, vol. 85, no. 9, pp. 1365–1388, 1997.
- [15] X. Li and S. Guo, *The Fourth Biometric-Vein Recognition*. Rijeka: InTech Open Access Publisher, 2008.
- [16] D. Lodrova, R. Dvovrak, M. Drahansky, and F. Orsag, "A new approach for veins detection," in *Bio-Science and Bio-Technology*. Heidelberg: Springer, 2009, pp. 76–80.
- [17] M. Deepamalar and M. Madheswaran, "An improved multimodal palm vein recognition system using shape and texture features," *International Journal of Computer Theory and Engineering*, vol. 2, no. 3, pp. 436-444, 2010.
- [18] M. Badawi, "Hand vein biometric verification prototype: a testing performance and patterns similarity," in *Proceedings of the 2006 International Conference on Image Processing, Computer Vision, & Pattern Recognition (IPCV)*, Las Vegas, NV, 2006, pp. 3-9.
- [19] A. Yuksel, L. Akarun, and B. Sankur, "Hand vein biometry based on geometry and appearance methods," *IET Computer Vision*, vol. 5, no. 6, pp. 398–406, 2011.
- [20] Y. Elmir, Z. Elberrichi, and R. Adjoudj, "Multimodal biometric using a hierarchical fusion of a person's face, voice, and online signature," *Journal of Information Processing Systems*, vol. 10, no. 4, pp. 555-567, 2014.
- [21] A. Nadort, "The hand vein pattern used as a biometric feature," Master Literature Thesis of Medical Natural Sciences at the Free University, Amsterdam, 2007.
- [22] K. Jain, P. Flynn, and A. A. Ross, *Handbook of Biometrics*. Boston, MA: Springer Science & Business Media, 2007.
- [23] S. Benziane and A. Benyettou, "Biometric technology based on hand vein," *Oriental Journal of Computer Science and Technology*, vol. 6, no. 4, pp. 401-412, 2013.
- [24] T. Nakazawa and K. Yazumi, "Biometric information registration apparatus and method," EP Patent 1,744,264, Dec. 18, 2013.
- [25] L. Wang and G. Leedham, "A thermal hand vein pattern verification system," in *Pattern Recognition and Image Analysis*. Heidelberg: Springer, 2005, pp. 58–65.
- [26] L. Y. Koon, "Implementation of hand vein biometric authentication on FPGA-based embedded system," Universiti Teknologi Malaysia, 2010.
- [27] L. Hanini and L. Limam, "Mise au point d'un système d'acquisition biométrique: SAB-11 Veines de la main," Institute of Maintenance and Industrial Safety, University of Oran, 2011.
- [28] J. G. Wang, W. Y. Yau, A. Suwandy, and E. Sung, "Person recognition by fusing palmprint and palm vein images based on "Laplacianpalm" representation," *Pattern Recognition*, vol. 41, no. 5, pp. 1514–1527, 2008.
- [29] L. Wang, G. Leedham, and S. Y. Cho, "Infrared imaging of hand vein patterns for biometric purposes," *IET Computer Vision*, vol. 1, no. 3, pp. 113–122, 2007.
- [30] L. Wang, G. Leedham, and S. Y. Cho, "Minutiae feature analysis for infrared hand vein pattern biometrics," *Pattern Recognition*, vol. 41, no. 3, pp. 920–929, 2008.
- [31] D. Saptono, "Conception d'un outil de prototypage rapide sur le FPGA pour des applications de traitement d'images," Ph.D. thesis, Université de Bourgogne, 2011.
- [32] M. Badawi, "Hand vein biometric verification prototype: a testing performance and patterns similarity," in *Proceedings of the 2006 International Conference on Image Processing, Computer Vision, & Pattern Recognition (IPCV)*, Las Vegas, NV, 2006, pp. 3-9.

- [33] K. Wang, Y. Zhang, Z. Yuan, and D. Zhuang, "Hand vein recognition based on multi supplemental features of multi-classifier fusion decision," in *Proceedings of the 2006 IEEE International Conference on Mechatronics and Automation*, Luoyang, China, 2006, pp. 1790–1795.
- [34] R. D. Prasanna, P. Neelamegam, S. Sriram, and N. Raju, "Enhancement of vein patterns in hand image for biometric and biomedical application using various image enhancement techniques," *Procedia Engineering*, vol. 38, pp. 1174–1185, 2012.
- [35] A. Fathima, S. Vasuhi, N. N. Babu, V. Vaidehi, and T. M. Treesa, "Fusion framework for multimodal biometric person authentication system," *IAENG International Journal of Computer Science*, vol. 41, no. 1, pp. 18–31, 2014.
- [36] L. Lin and K. C. Fan, "Biometric verification using thermal images of palm-dorsa vein patterns," *IEEE Transactions on Circuits and Systems for Video Technology*, vol. 14, no. 2, pp. 199–213, 2004.
- [37] E. Makimoto, K. Nomura, Y. Mizuno, N. Takamura, and H. Ogata, "Biometric authentication apparatus and biometric authentication method," EP20,100,187,628, Apr. 20, 2011.
- [38] S. Malki and L. Spaanenburg, "Hand veins feature extraction using DT-CNNs," in *Microtechnologies for the New Millennium*. Bellingham, WA: International Society for Optics and Photonics, 2007, pp. 65900N–65900N.
- [39] A. Kong, D. Zhang, and M. Kamel, "A survey of palmprint recognition," *Pattern Recognition*, vol. 42, no. 7, pp. 1408–1418, 2009.
- [40] T. Tanaka and N. Kubo, "Biometric authentication by hand vein patterns," in *Proceedings of SICE 2004 Annual Conference*, 2004, pp. 249–253.
- [41] A. Mostayed, M. E. Kabir, S. Z. Khan, M. M. G. Mazumder, "Biometric authentication from low resolution hand images using radon transform," in *Proceedings of 12th International Conference on Computers and Information Technology*, Chengdu, China, 2009, pp. 587–592.
- [42] S. Hama, T. Aoki, and M. Fukuda, "Biometric authentication device and biometric authentication method," EP20,080,878,913, Oct 5, 2011.
- [43] A. Kumar and K. V. Prathyusha, "Personal authentication using hand vein triangulation and knuckle shape," *IEEE Transactions on Image Processing*, vol. 18, no. 9, pp. 2127–2136, 2009.
- [44] M. Monwar, S. Rezaei, and K. Prkachin, "Eigenimage based pain expression recognition," *IAENG International Journal of Applied Mathematics*, vol. 36, no. 2, pp. 1–6, 2007.
- [45] S. Benziane and A. Benyettou, "State of art: hand biometric," *International Journal of Advances in Engineering & Technology*, vol. 2, no. 1, 2012.
- [46] S. Benziane and A. Benyettou, "An introduction to biometrics," *International Journal of Computer Science and Information Security*, vol. 9, no. 4, pp. 40–47, 2011.
- [47] L. Lin, Y. Cong, and Y. Tang, "Hand gesture recognition using RGB-D cues," in *Proceedings of 2012 International Conference on Information and Automation (ICIA)*, Shenyang, China, 2012, pp. 311–316.
- [48] S. K. Im, H. M. Park, Y. W. Kim, S. C. Han, S. W. Kim, C. H. Kang, and C. K. Chung, "An biometric identification system by extracting hand vein patterns," *Journal-Korean Physical Society*, vol. 38, no. 3, pp. 268–272, 2001.
- [49] R. Stewart, "Security enhanced blasting apparatus with biometric analyzer and method of blasting," EP20,110,165,738, Aug. 17, 2011.
- [50] S. Benziane and A. Benyettou, "Biometric technology based on hand vein," *Oriental Journal of Computer Science and Technology*, vol. 6, no. 4, pp. 401–412, 2013.
- [51] S. H. Benziane and A. Benyettou, "Anisotropic diffusion filter for dorsal hand vein features extraction," *International Journal of Biology and Biomedicine*, vol. 1, pp. 27–31, 2016.
- [52] A. Jagadeesan, T. Thillaikkarasi, and K. Duraiswamy, "Cryptographic key generation from multiple biometric modalities: fusing minutiae with iris feature," *International Journal of Computer Applications*, vol. 2, no. 6, pp. 16–26, 2010.



### Sarah Hachemi Benziane

She is assistant professor in computer science; she obtained her magister electronics about mobile robotics. She holds a basic degree from computer science engineering. Now, she's working with biometrics system's processing in SMPA laboratory, at the university of Science and Technology of Oran Mohamed Boudiaf (Algeria). She teaches at the University of Oran at the Maintenance and Industrial Safety Institute. Her current research interests are in the area of artificial intelligence and image processing, mobile robotics, neural networks, Biometrics, neuro-computing, GIS and system engineering.



### Abdelkader Benyettou

He received the engineering degree in 1982 from the Institute of Telecommunications of Oran and the M.Sc. degree in 1986 from the University of Sciences and Technology of Oran-USTO, Algeria. In 1987, he joined the Computer Sciences Research Center of Nancy, France, where he worked until 1991 on Arabic speech recognition by expert systems (ARABEX) and received the PhD in electrical engineering in 1993 from the USTO University. From 1988 to 1990, he has been an assistant Professor in the department of Computer Sciences, Metz University, and Nancy-I University. He is actually professor at the USTO University since 2003. He is currently a researcher director of the Signal-Speech-Image-SIMPA Laboratory, department of Computer Sciences, Faculty of sciences, USTO, since 2002. His current research interests are in the area of speech and image processing, automatic speech recognition, neural networks, artificial immune systems, genetic algorithms, neuro-computing, machine learning, neuro-fuzzy logic and handwriting recognition.